Supporting Information

Intermediate Phase Halide Exchange Strategy toward High-Quality, Thick $CsPbBr_3$ Film for Optoelectronic Application

Weidong Zhu,[a,‡,*] Minyu Deng,[a,‡] Zeyang Zhang,[a,‡] Dazheng Chen,[a] He Xi,[a,b] Jingjing Chang,[a] Jincheng Zhang,[a] Chunfu Zhang,[a,*] Yue Hao[a]

[a]State Key Discipline Laboratory of Wide Band Gap Semiconductor Technology & Shaanxi Joint Key Laboratory of Graphene, School of Microelectronics, Xidian University, Xi'an, 710071, China.

[b]State Key Laboratory of Crystal Materials, Shandong University, Jinan, 250100, China.

E-mail: wdzhu@xidian.edu.cn, cfzhang@xidian.edu.cn

‡These authors contributed equally to the work.

EXPERIMENTAL SECTION

Reagents and materials: Ultradry $PbBr_2$ (99.999%, AlfaAesar), ultradry CsI (99.998%, Alfa-Aesar), CH_3NH_3Br (≥99.5%, Xi'an Polymer Light Technology Corp.), anhydrous MeOH (99.9%, Alfa-Aesar), DMSO (ACS reagent, ≥99.9%, Sigma-Aldrich), conductive carbon paste (ZF-G03- 04-2, Shanghai MaterWin New Materials Co., Ltd.), and FTO glass (TEC8, 8 Ω sq^{-1}, Pilkington TEC Glass) were purchased and used as received unless otherwise noted.

Fabrication of $CsPbBr_3$ film photodetector. FTO glass was cleaned in an ultrasonic bath sequentially with detergent, deionized water, acetone, and alcohol for 15 min, respectively. A ~60 nm compact TiO_2 layer was then coated onto FTO glass by spin-coating TiO_2 sol at 3500 rpm for 30 s, followed by annealing in air at 500 °C for 60 min. Thus, the FTO/TiO_2 substrate was obtained. To form CsI-$PbBr_2$-DMSO intermediate phase film, 370 mg $PbBr_2$ and 260 mg CsI were fully dissolved in 1 mL DMSO at room temperature to form the precursor, and then 70 μL precursor was coated onto FTO/TiO_2 substrate at 2500 rpm for 30 s, and 5000 rpm for 120 s. For halide exchange, a certain volume (typical 60 μL) of MeOH solution containing of 20 mg mL^{-1} CH_3NH_3Br was spin-coated onto the intermediate phase film at 5000 rpm for 30 s. The sample was preheated at 80 °C for 5 min to promote full halide exchange and evaporation of some DMSO solvent molecules, and it was further annealed at the optimized temperature of 300 °C for 10 min. After that, the $CsPbBr_3$ film was achieved successfully. Finally, a carbon electrode with the area of 0.09 cm^2 was deposited onto $CsPbBr_3$ film by silkscreen-printing of conductive carbon paste, in order to fulfill the fabrication of photodetector.

Characterizations of $CsPbBr_3$ film and photodetector. XRD measurements were conducted with a Bruker D8 Advance Davinci powder X-ray diffractometer using a Cu K_α radiation (1.5406Å). Absorption spectra were measured by UV-vis/NIR spectrophotometer (U-4100, Hitachi). Surficial and cross-sectional morphology of $CsPbBr_3$ film was studied by a high-resolution SEM (JEOL-7100F). AFM was performed by a Bruker multimode 8 in 'tapping' mode. Micro-Raman measurements were carried out using a Horiba HR800 Raman system at room temperature with a 514 nm laser excitation. J–V curves of the photodetectors were measured by a Keithley 2450 source meter. Light source was provided by a Xenon lamp power supply. EQE spectra were collected on a Zolix DSR-101-UV system equipped with a Si PD as reference. Photoresponsibility (R) values of device can be obtained via the relationship:[1] $R = \frac{\lambda \cdot EQE}{hc/e} = \frac{\lambda \cdot EQE}{1.24 \times 10^{-6}} A/W$, where λ is the wavelength, h is the Plank constant, c is the light speed, and e is the elementary charge. The random fluctuation of electrons caused by thermal excitation is called shot noise, which is the main noise source of photovoltaic thin film photoconductance. For photodetectors that shot noise is the main noise source, equivalent noise power can be expressed as: $NEP = \frac{\sqrt{2 \cdot e \cdot I_d . \Delta f}}{R}$. And, because of $D = \frac{1}{NEP}$ and $D^* = D\sqrt{A \cdot \Delta f}$, so we can deduce the relationship:[2,3] $D^* = \frac{R\sqrt{A}}{\sqrt{2 \cdot e \cdot I_d}}$, where A is the device working area, e is the elementary charge and I_d is the measured dark current. TPC curves were recorded by a digital oscilloscope (Tektronix, MSO5204B) with an input resistance of 50 Ω, when the device was illuminated with a 520 nm pulse laser (MDL-NS-520). The entire characterizations are finished in ambient air conditions.

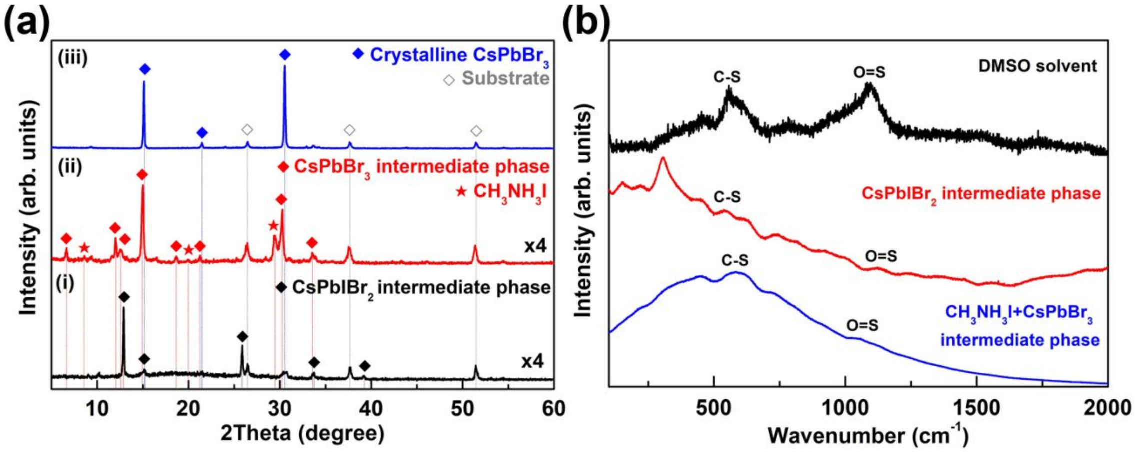

Figure S1. (a) XRD patterns of (i) $CsPbIBr_2$ intermediate phase film, (ii) CH_3NH_3I+$CsPbBr_3$ intermediate phase film, and (ii) crystalline $CsPbBr_3$ film, respectively. The diffraction peaks of CH_3NH_3I species can be detected from the CH_3NH_3I+$CsPbBr_3$ intermediate phase film. (b) Raman spectra of DMSO solvent, $CsPbIBr_2$ intermediate phase film, and CH_3NH_3I+$CsPbBr_3$ intermediate phase film.

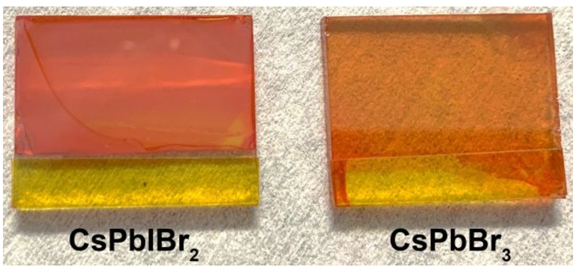

Figure S2. Optical photographs of the resultant films without and with halide exchange procedure. The former can be assigned to $CsPbIBr_2$, while the latter is $CsPbBr_3$.

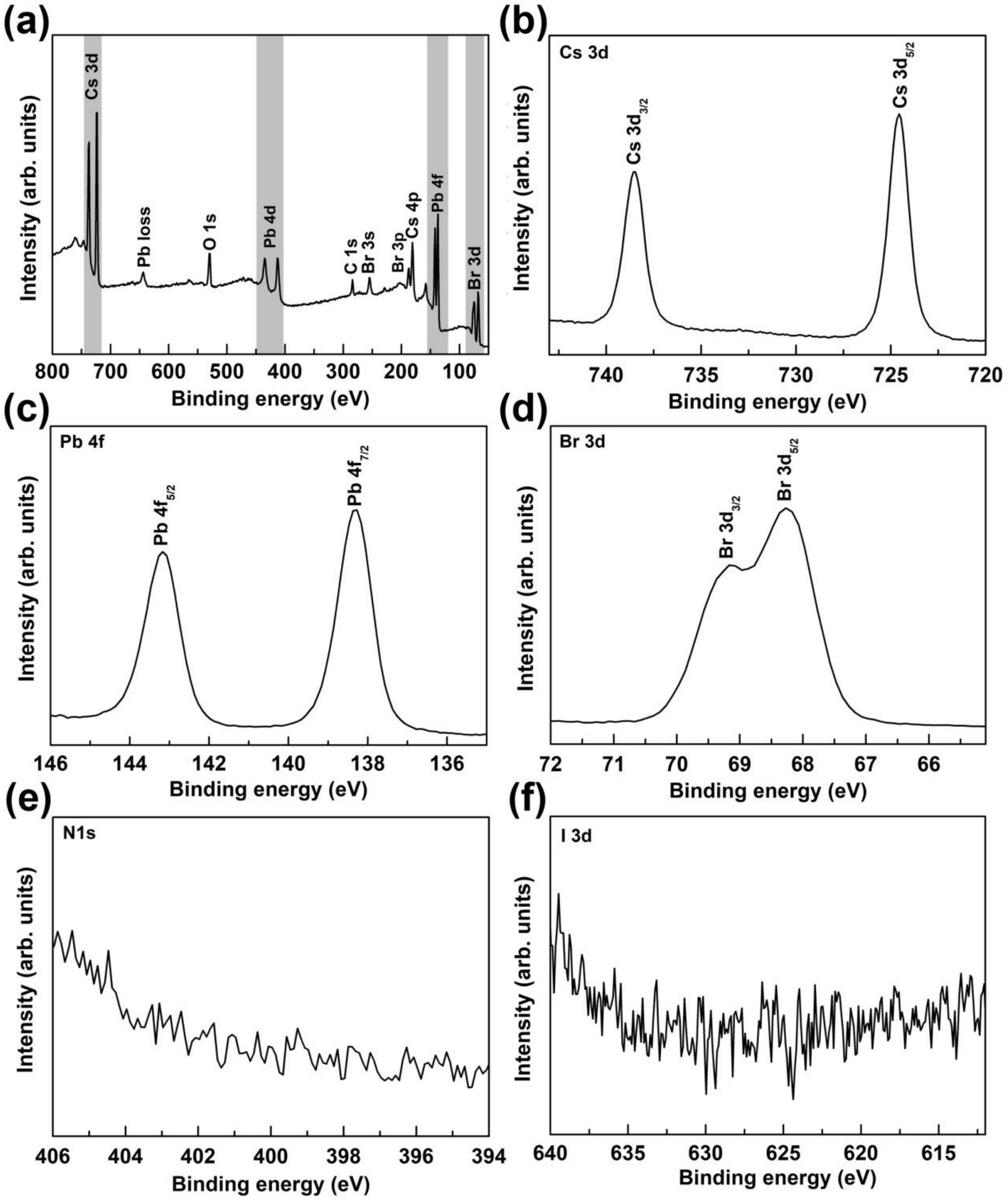

Figure S3. (a) XPS survey spectrum of $CsPbBr_3$ film prepared with 60 μL CH_3NH_3Br solution. The film was annealed at 200 ^oC for 10 min. (b) Cs 3d, (c) Pb 4f, (d) Br 3d, (e) N 1s, and (f) I 3d XPS core spectra for the same film.

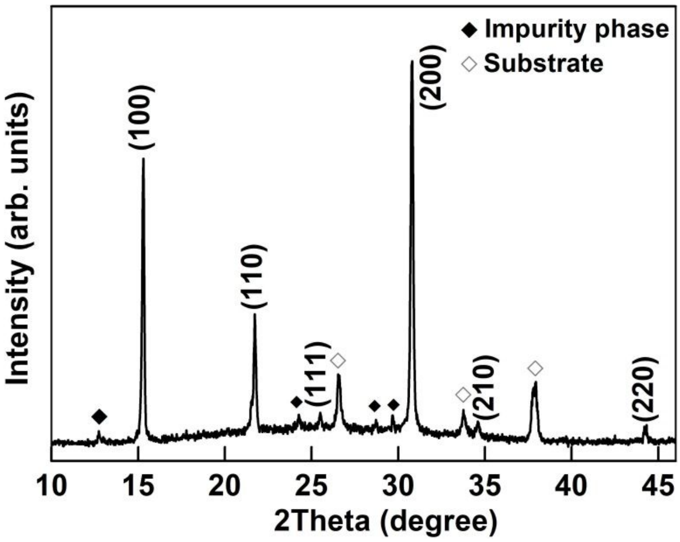

Figure S4. XRD pattern of $CsPbBr_3$ film annealed at 350 ^{o}C for 10 min.

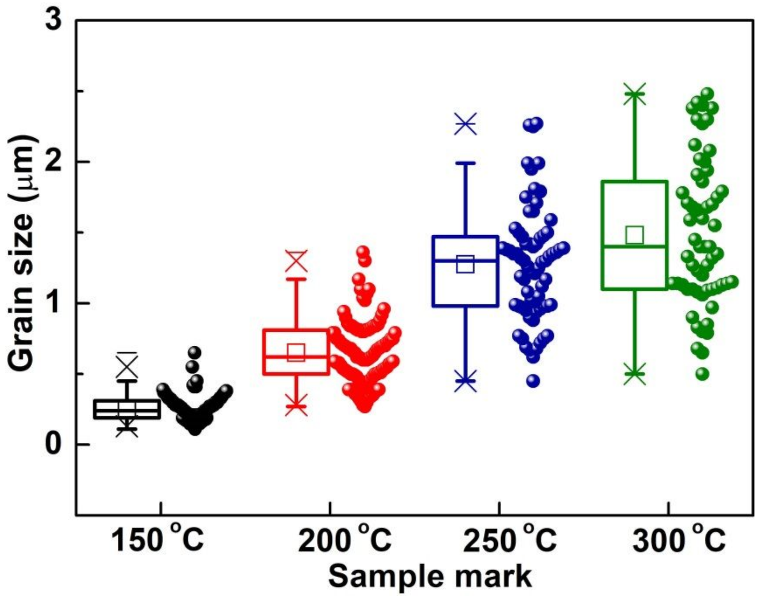

Figure S5. Box charts of grain sizes of $CsPbBr_3$ films annealed at 150, 200, 250, and 300 ^{o}C, respectively.

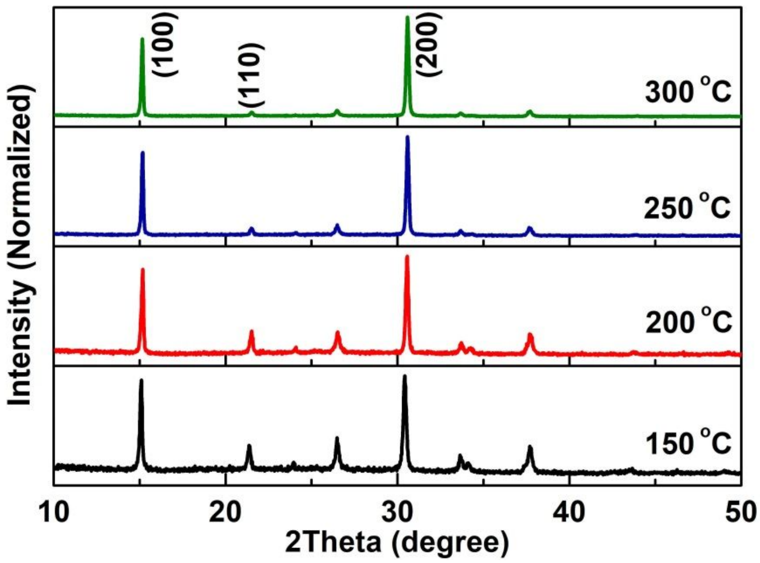

Figure S6. Normalized XRD patterns of $CsPbBr_3$ films annealed at 150, 200, 250, and 300 °C, respectively.

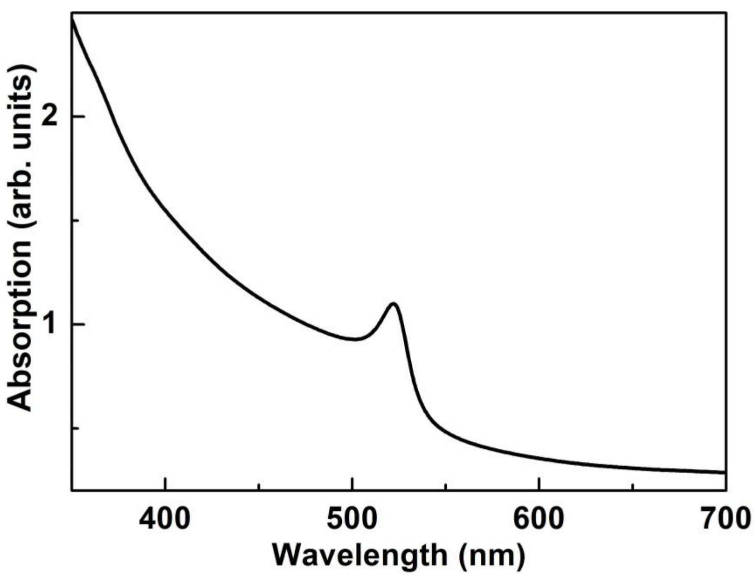

Figure S7. Absorption spectrum of $CsPbBr_3$ film annealed for a prolonged time of 1 h at 150 °C.

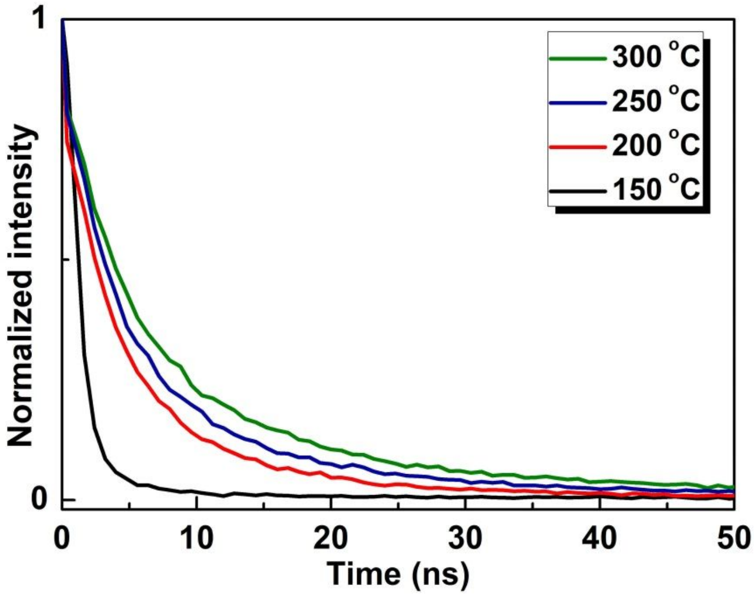

Figure S8. PL decay curves of the $CsPbBr_3$ films annealed at 150, 200, 250, and 300 ^{o}C, respectively. The films are deposited on insulated glass substrates.

Table S1. Summary of peak responsivities and D* values for $CsPbBr_3$-based photodetectors with vertical structure.

Cell configuration	Bias (V)	Responsivity (A/W)	D* (Jones)	Reference
$FTO/TiO_2/CsPbBr_3$/Carbon	0	0.35	1.94×10^{13}	**This work**
$ITO/SnO_2/CsPbBr_3$ microcrystals/Spiro-MeOTAD/Au	0	0.172	4.80×10^{12}	[16]
ITO/PEALD-SnO_2/ $CsPbBr_3$ nanowires/PTAA/Au	0	0.3	1.0×10^{13}	[17]
ITO/PTAA/PEIE/$CsPbBr_3$/ PCBM/BCP	0	0.13	6.0×10^{12}	[40]
FTO/ZnO nanowires/ $CsPbBr_3/MoO_3$/Au	0	0.3	1.15×10^{13}	[43]

ITO/SnO_2/$CsPbBr_3$ microcrystals/ Spiro-MeOTAD/Au	0	0.206	7.23×10^{12}	[44]
ITO/$CsPbBr_3$:ZnO/Ag	0	0.0115	-	[45]

References

(1) Bao, C.; Yang, J.; Bai, S.; Xu, W.; Yan, Z.; Xu, Q.; Liu, J.; Zhang, W.; Gao, F. High Performance and Stable All-Inorganic Metal Halide Perovskite-Based Photodetectors for Optical Communication Applications. *Adv. Mater.* **2018,** *30*, 1803422.

(2) Tian, W.; Zhou, H.; Li, L. Hybrid Organic–Inorganic Perovskite Photodetectors. *Small* **2017,** *13*, 1702107.

(3) Dong, Y.; Gu, Y.; Zou, Y.; Song, J.; Xu, L.; Li, J.; Xue, J.; Li, X.; Zeng, H. Improving All-Inorganic Perovskite Photodetectors by Preferred Orientation and Plasmonic Effect. *Small* **2016,** *12*, 5622.